ENVIRONMENTAL FATE OF POLYCYCLIC AROMATIC HYDROCARBONS IN NAGOYA PORT

Student Number: 06M16040 Name: Hiroyuki OKUMURA Supervisor: Taro URASE

名古屋港における多環芳香族炭化水素類の環境動態に関する研究

奥村　浩幸

本研究では，港湾域で注目される化学物質である多環芳香族炭化水素類（PAHs）の環境動態を把握するため，名古屋港での現地観測，名古屋港港湾堆積物を用いた PAHs の吸着・脱着・分解実験を行った．またマスバランスモデルを適用し，名古屋港における PAHs の環境動態について検討を行った．PAHs の粒子吸着特性は堆積物中有機物との分配係数 K_{oc} で表現でき，一方脱着は起こり難いことがわかった．堆積物中の分解速度は無視し得るほど遅く，分子量の大きい PAHs ほど港外への流出が少なく，堆積物への移行が多いことがわかった．

Key Word: *Polycyclic Aromatic hydrocarbons, sediment, adsorption, desorption, degradation*

1. INTRODUCTION

Polycyclic aromatic hydrocarbons, called PAHs, were widely distributed in environments with human activities such as burning of fossil fuel. For instance, Benzo(a)pyrene, one of PAHs, is a strong mutagen and carcinogen , and some of PAHs metabolites have endocrine disruption activity [1][2]. Therefore, studying PAHs concentration levels and fate in environments is important to assessing PAHs exposure to organisms including human being.

Physical-chemical properties of PAHs vary widely by their ring-number. The higher ring-number PAHs have higher hydrophobicity, the lower vapor pressure and higher toxicity. In general, PAHs with high ring-numbers, adsorb to fine particles due to there high hydrophobicity, and behave like particle [3]. After PAHs are discharged to the atmosphere from burning of fossil fuel etc, the deposition of PAHs occurs to land surface with fine particles, before the accumulation on road surface etc. The particles flow into rivers by runoff, eventually are transferred to sediments of lakes, bays, harbors and ports [4]. Consequently, organisms in aqueous environments were also exposed to PAHs adsorbed onto fine particles.

In Japan, PAHs are not listed in the environmental quality standard. PAHs were detected at high levels in sediments of ports and harbors, where chemical compounds are transferred by dredging and soil capping.

In this study, to clarify the environmental fate of PAHs, field observations in Nagoya port was conducted together with adsorption, desorption and degradation experiments in aerobic and anaerobic conditions by using sediments obtain from Nagoya port. Mass balance model was applied to the data from field observation and laboratory experiments to consider the environmental fate of PAHs in Nagoya port.

2. FIELD OBSERVATION

(1) Outline of the field observation

The field observation in Nagoya port was conducted on May 2007. The port area is 83 km^2. The average difference of tidal level is 1.3 m. **Fig. 1** shows four sampling points. St. A was at the end of the port, and St. D was outside of breakwater. St. A, B, C was in highly industrialized area. The major river flow into the port is the Tenpaku River, and St. C was influenced by the river. 10 cm sediment core samples were collected at St. A to D. The 10 cm sediment core was divided into 5 layers with the thickness of 2 cm. PAHs concentration, particles size distribution, moisture content, ignition loss, density of solids, total organic carbon content and total organic nitrogen content were measured. **Table 1** shows the soil properties of the sediment core samples.

(2) The analysis method of PAHs

PAHs concentration in solid phase was measured by heating with the alkaline solvent extraction method. Approximately 1.0 g-wet sediment was added to 20 mL of ethanol and 1.0 g of potassium hydroxide. PAHs internal standard solution was added for internal standardization, and heated at 70 ℃ for 60 min, and sonicated for 5 min. After a 5 minutes centrifugation at 3000 rpm,

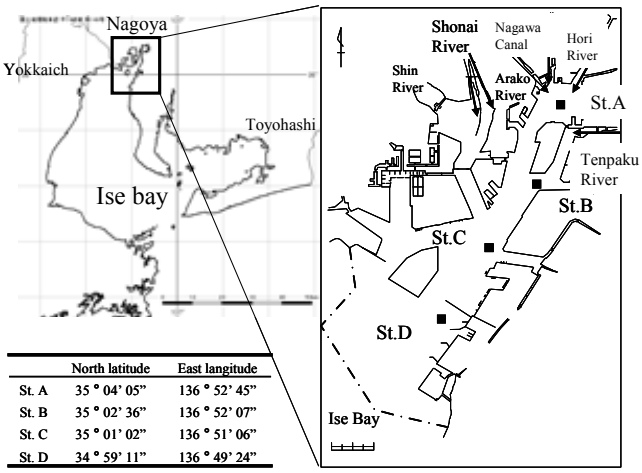

	North latitude	East langitude
St. A	35 ° 04' 05"	136 ° 52' 45"
St. B	35 ° 02' 36"	136 ° 52' 07"
St. C	35 ° 01' 02"	136 ° 51' 06"
St. D	34 ° 59' 11"	136 ° 49' 24"

Fig. 1 Sampling points of sediment core samples

Table 1 Soil properties of sediment core samples

		Moisture cotent [%]	Ignition loss [%]	Density [g/cm^3]	TOC [mg/g]	TON [mg/g]
St.A	0-2cm	78.5	15.6	2.513	38.4	4.18
	2-4cm	79.2	17.2	2.465	36.8	3.90
	4-6cm	81.2	21.1	2.516	35.0	3.49
	6-8cm	78.6	17.0	2.532	34.7	3.59
	8-10cm	78.5	17.3	2.516	36.1	3.52
St.B	0-2cm	58.2	10.9	2.622	31.8	1.99
	2-4cm	58.4	11.1	2.611	32.9	1.91
	4-6cm	60.7	11.3	2.627	31.7	1.91
	6-8cm	59.3	10.9	2.632	32.3	1.72
	8-10cm	58.8	11.4	2.621	33.7	1.90
St.C	0-2cm	60.6	10.0	2.606	21.9	2.16
	2-4cm	59.3	9.5	2.638	19.8	1.91
	4-6cm	59.7	10.4	2.586	20.4	1.96
	6-8cm	60.6	10.1	2.616	20.1	1.88
	8-10cm	60.4	10.4	2.589	20.2	1.91
St.D	0-2cm	42.9	7.8	2.674	16.0	1.07
	2-4cm	35.3	9.2	2.668	13.7	0.91
	4-6cm	35.2	8.4	2.674	11.7	0.85
	6-8cm	32.1	7.5	2.670	14.7	0.86
	8-10cm	31.3	8.7	2.678	13.1	0.80

Table 2 Physical-chemical properties of PAHs

Name	abbr.	Number of rings	Molecular weight [g/mol]	Density [g/cm^3]	Melting point [℃]	Boiling point [℃]	Solubility [mg/L]	Log Kow
Naphthalene	Nap	2	128	1.16	80.2	218.0	30.7	3.37
Acenaphthylene	Acl	3	152	0.90	92.5	270.0	-	4.00
Acenaphthene	Ace	3	154	1.05	96.2	278.0	4.47	3.92
Fluorene	Flu	3	166	1.20	116.0	295.0	1.99	4.32
Phenanthrene	Phe	3	178	0.98	101.0	339.0	0.0659	4.57
Anthracene	Ant	3	178	1.25	217.5	341.0	1.28	4.45
Fluoranthene	FR	4	202	1.25	110.5	384.0	0.263	5.22
Pyrene	Pyr	4	202	1.27	156.0	403.0	0.145	5.18
1,2-Benzanthracene	BaA	4	228	1.25	160.6	437.5	-	5.61
Chrysene	Chr	4	228	1.28	255.0	448.0	0.00296	5.91
Benzo(b)fluoranthene	BbF	5	252	-	-	-	-	6.12
Benzo(k)fluoranthene	BkF	5	252	-	-	-	-	6.08
Benzo(a)pyrene	BaP	5	252	-	176.5	496.0	0.00378	6.35

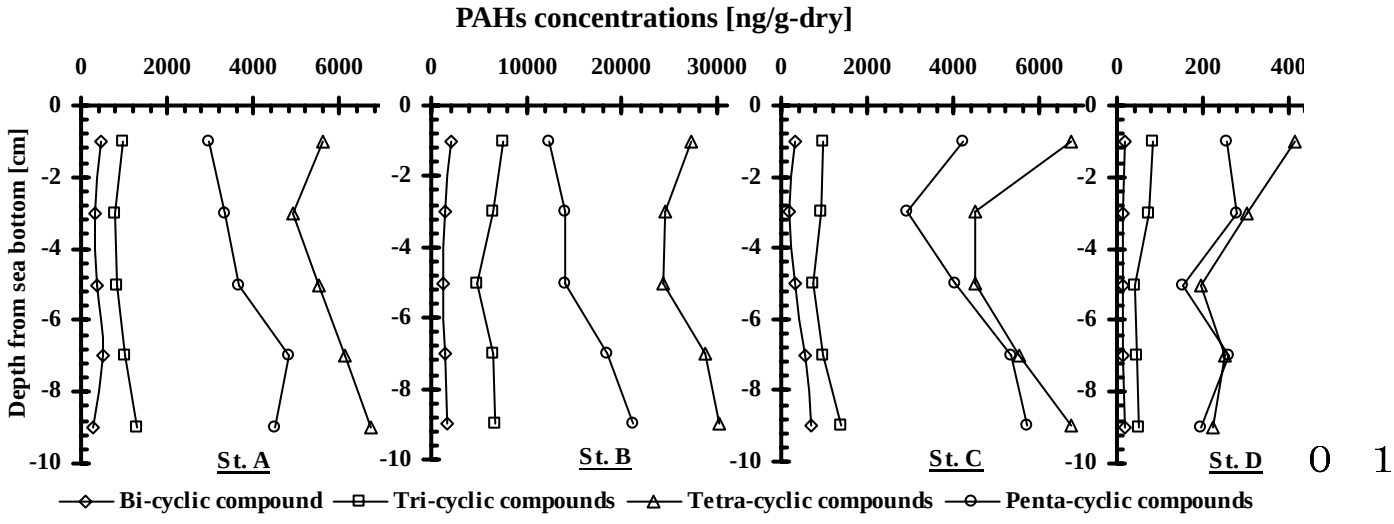

Fig. 2 Vertical distribution of PAHs concentrations at St. A to D

the ethanol solution was decanted to a separating funnel. 10 mL of hexane was poured into the funnel, and then shaken for 5 min. The extracted hexane solution was concentrated under 60 ℃ with nitrogen gas stream. The concentrated solution was then analyzed by a GC/MS. Target compounds were 13 PAHs as shown in **Table 2**.

(3) Results and discussion

Fig. 2 shows the vertical distributions of PAHs concentrations at St. A to D, plotted with the summation of the same ring-number compounds. Tetra-cyclic and penta-cyclic compounds were detected with higher concentration rather than bi-cyclic and tri-cyclic compounds in the case of all sampling points. Although PAHs concentrations slightly increased with depth, overall PAHs concentrations were similar range with depth. Taking the sedimentation rate (1.4cm/year) [5] into account, the external loading of PAHs was a constant in these 7 years.

Fig. 3 shows PAHs concentrations at St. A to D averaged with depth. Total PAHs concentrations ($\sum_{13}$PAHs) were 11000 ng/g-dry at St. A, 51000 ng/g-dry at St. B, 11500 ng/g-dry at St. C and 580 ng/g-dry at St. D. Although distance from St. A to B was 4 km, $\sum_{13}$PAHs at St. B was five times higher than that at St. A. Thus, depositions due to point sources near the sampling point influenced at St. B rather than atmospheric diffusive transport. The total PAHs concentration was compared with previous studies, though number of target compounds was different. $\sum_{15}$PAHs of 189-637 ng/g-dry was observed at the Pear river estuary [6], $\sum_{13}$PAHs 180-960 ng/g-dry at coastal wetland in Hong Kong [7], $\sum_{17}$PAHs 100-795 ng/g-dry at Lake Suwa [8], $\sum_{25}$PAHs 31-316 ng/g-TOC at San Francisco bay [9], $\sum_{16}$PAHs 38-2000 ng/gdry at Tokyo bay [10], $\sum_{10}$PAHs 53-26000 ng/g-dry at the moat in Osaka castle [11]. The observed concentration at St. B was in a dramatically high level.

National Oceanic and Atmospheric Administration (NOAA, U.S.) presented the value of ERL (effects range low) and ERM (effects range median) as the guideline of biological assessment

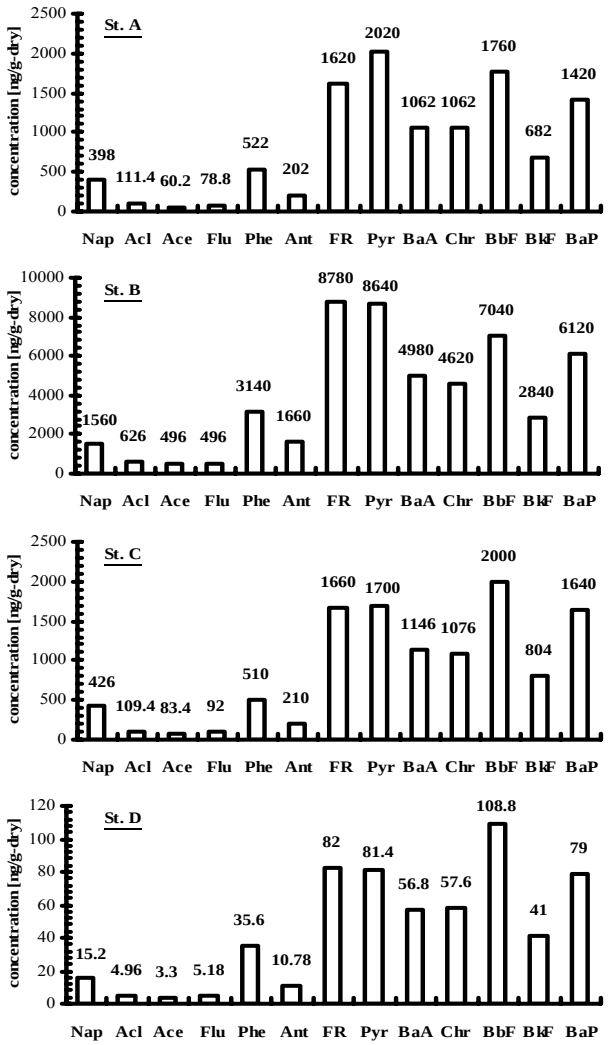

Fig. 3 Average PAHs concentrations at St. A to D

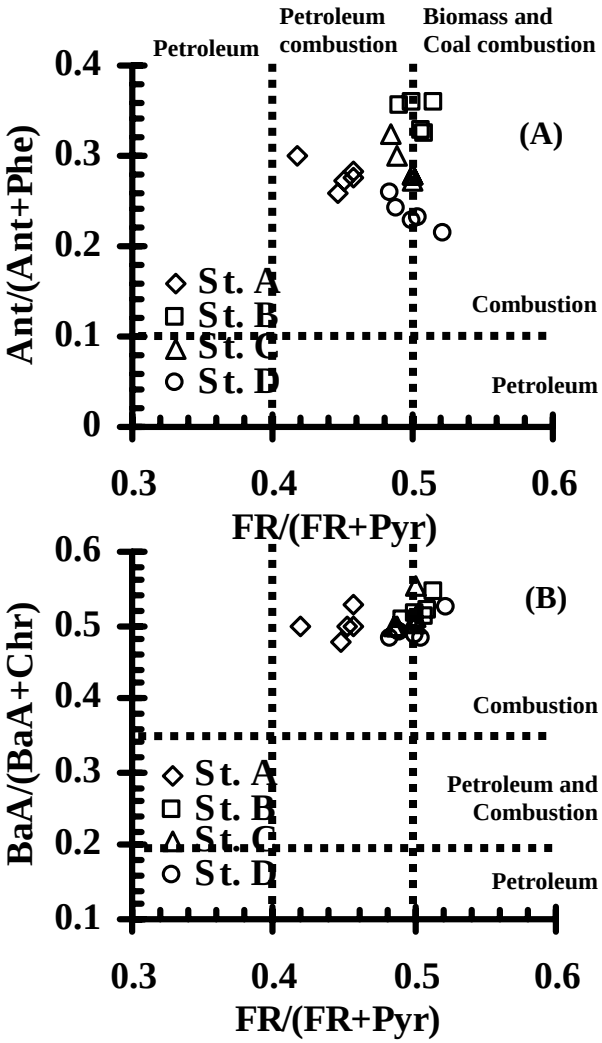

Fig. 4 Plots of PAHs isomer pair ratios for source identification.

[12]. NOAA identified the 10^{th} percentile and the 50^{th} percentile (median) of the occurrence frequency of adverse effects for each substance. The 10^{th} percentile values were named ERL, indicative of concentrations below which adverse effect rarely occur. The 50^{th} percentile values were named ERM, representative of concentrations above which effects frequently occur. The ERL value of total PAHs was 4022 ng/g, and the ERM value of total PAHs was 44792 ng/g. $\sum_{13}$PAHs at St. A and C were between ERL and ERM. $\sum_{13}$PAHs at St. B exceeded ERM, which indicates probable adverse effect on benthos.

The major sources of PAHs are the exhausts of diesel and gasoline engine vehicles, tires, and road materials [13][14]. It was reported previously that each source of PAHs has each characteristic pattern of a PAHs profile [7] and the usefulness of PAHs isomer ratios, such as Ant/(Phe+Ant), was demonstrated for the source identification. As phenanthrene is a thermodynamically more stable tri-cyclic aromatic isomer than anthracene, the Ant/(Phe+Ant) ratio has been frequently used to differentiate PAHs of petrogenic origin from those of pyrogenic origin in the environment. Petrogenic PAHs are generally characterized by a low ratio (normally <0.1) while those of pyrogenic origin possess higher ratio. Based on the PAHs measurements compiled by Yunker et al. [15]: Ant/(Ant+Phe) <0.10 indicates dominance of petroleum sources and >0.10 indicates the dominance of combustion sources; FR/(FR+Pyr) <0.40 indicates petroleum sources, 0.40-0.50 petroleum combustion sources, >0.50 biomass and coal combustion sources; BaA/ (BaA+Chr) <0.20 petroleum sources, 0.20-0.35 petroleum and combustion sources, >0.35 combustion sources. PAHs isomer pair ratios were plotted against FR/(FR+Pyr) to show how PAHs distribute relative to their possible sources (**Fig. 4**). An Ant/(Ant+Phe) ratio >0.10 indicates that 2-3 ring volatile PAHs in 100% of Nagoya port sediments are derived from combustion. The sediment samples with a BaA/ (BaA+Chr) isomer pair ratio of > 0.35 suggest that 4-6 ring non-volatile PAHs are derived from primarily from combustion sources. A FR/(FR+Pyr) ratio 0.42-0.46 at St. A indicates the dominance of petroleum combustion at St. A. In contrast, the ratio 0.48-0.51 at St. B, C, and D indicates the mixed source of petroleum combustion and biomass and coal combustion. Because the ratio at St. A obviously differed from St. B, C and D, different sources were suspected for the sample at St. A.

3. LABORATORY EXPERIMENTS

Experiments of adsorption, desorption and degradation in anaerobic and aerobic condition of PAHs using Nagoya port sediment were conducted.

(1) Materials and methods

a) Adsorption experiment

The sediments of St. A to D were used to the adsorption experiment. Batch reaction systems with 0.5 g-wet sediment and 50 mL artificial sea water were used for the experiment. The sediment was diluted to 50 mL with the artificial sea water, and 20 mg/L PAHs standard solution of 100 μL was added with the initial concentration was 40 μg/L. Then the slurry stirred at 160 rpm for 5 min, 1 hr, 24 hr and 48 hr, respectively. The experiments were run in the dark and at a constant temperature (25 ± 1 ℃) to minimize possible losses by photodegradation and evaporation. After stirred, the slurry was centrifuged at 3000 rpm at 5 min. The supernatant liquid was filtered with the glass fiver filter (1 μm), and the dissolved phase was separated from the solids phase. PAHs concentrations in dissolved phase (C_w) and solid phase (C_s) were then analyzed, and partition coefficient ($K_p=C_s/C_w$) was calculated. Control experiments without solids were performed in the same manner.

b) Desorption experiment

The sediment of St. B was used to the desorption experiment. Batch reaction systems with 10 g-wet sediment and 50 mL artificial sea water were used for the experiment. The sediment was diluted to 50 mL with the artificial sea water, and stirred at 160 rpm for 5 min, 1 hr, 24 hr, 8 day and 21 day, respectively. The experiments were conducted in the dark and at a constant temperature (25 ± 1 ℃) to minimize possible losses by photodegradation and evaporation. After stirred, the slurry was centrifuged at 3000 rpm at 5 min. The supernatant liquid were filtered with the glass fiver filter (1 μm), and dissolved phase were separated from the solids phase. PAHs concentrations in dissolved phase and solid phase were then analyzed, and partition coefficient was calculated. Control experiments without solids were performed in the same manner.

c) Anaerobic degradation experiment

The sediments of St. A to D were used to the degradation experiment in an anaerobic condition (moisture content: 32.5-78.8%). The marine sediments at the surface of the core samples were stored at 25 and 40 ℃ in anaerobic condition, respectively. 100 and 180 days later, PAHs concentration changes in the sediment were measured.

d) Aerobic degradation experiment

The sediment of St. B was used to the degradation experiment in an aerobic condition. Batch reaction systems with 5 g-wet sediment and 50 mL artificial sea water and the Tamagawa river water were used for the experiment. The sediments were diluted to 50 mL with the artificial sea water and Tamagawa river water, respectively. The slurries were stirred with 110 rpm to make aerobic condition at 25 ℃. 30 and 60 days later, PAHs concentration changes in the sediment were measured.

e) The analysis method of PAHs

PAHs concentration in solid phase was measured by heating with the alkaline solvent extraction method as above. PAHs concentration in dissolved phase was measured as follows. The filtrated solution was decanted to separating funnel. 10 mL of Hexane was pored into the funnel, and PAHs internal standard solution was added for internal standardization, and then shaken for 5 min. The extracted hexane solution was concentrated under 60 ℃ with nitrogen gas stream. The concentrated solution was then analyzed by a GC/MS.

(2) Results and discussion

Fig. 5 shows the plots of Log K_p against Log K_{ow} with various stirred period in adsorption experiment. The hydrophobic compounds had the higher K_p i.e. more partition in solid phase. Hydrophobic compounds that have more than 4 rings adsorbed to sediments more than 50% within 5 min. After that, K_p gradually increased with time. K_p differed slightly from 1hr to 48 hr compared with the initial to 5 min. It was assumed that adsorption equilibrium was reached with 24 hr.

Fig. 6 shows the plots of Log K_p against Log K_{ow} at St. A to D in adsorption experiment. There was a clear correlation between K_p and K_{ow}. K_p at St. A and B were higher than St. C, and K_p of St. D was lowest. PAHs tended to more adsorb to organic-rich sediments.

Water-ignition loss partition coefficient (K_{om}= K_p/*IL*) and water-TOC partition coefficient (K_{oc}= K_p/*TOC*) were calculated, and summarized as shown in **Table 3**.

Fig. 7 shows the plots of Log K_{oc} against Log K_{ow} at St. A to D in adsorption experiment. K_{oc} had a higher correlation with K_{ow} than K_{om} and K_p. By using K_{oc}, differences with sediments became smaller. An expression for the relation between K_{oc} and K_{ow} was obtainede as follow.

$$\mathrm{Log}_{10}K_{oc}=1.23\cdot\mathrm{Log}_{10}K_{ow}-1.05 \quad (1)$$

In addition, as well as TOC, K_p was influenced by specific surface area of sediments. K_{oc} at St. D was lowest, and St. D had low fine particle fraction content of 62% compared to St. A, B and C where the fine particle fraction was between 92-96%. It was suspected adsorption capacity was affected by specific surface area of sediments.

Fig. 8 shows differences of K_p between adsorption and desorption experiments. K_p obtained from desorption experiment was 30-100 times greater than that obtained from the adsorption experiment. Dissolved concentrations of hydrophobic compounds that have more than 5 rings were below the detection limits. In the adsorption experiment, the equilibrium was reached within 1hr (**Fig. 5**). On the other hand, in the desorption experiment, desorption continued after 24hr, and K_p decreased with time. Therefore, PAHs that once adsorbed to sediments would not be released from the sediments, even if sediments were diluted in sea water due to resuspension.

Fig. 9 and 10 show PAHs concentration changes at St. B and C in the anaerobic degradation experiment. Although Fluoranthene (FR) and Pyrene (Pyr) were slightly decreased in the case of samples taken at St. B and C, overall PAHs concentrations did not decrease significantly enough to calculate the degradation rate.

Fig. 11 shows PAHs concentration changes at St. B in the aerobic degradation experiment. As well as in the case of the anaerobic degradation experiments, PAHs concentrations did not decrease significantly enough to calculate degradation rate in the aerobic degradation experiment.

Several previous studies [16][17][18][19][20] reported on the degradability of PAHs. Certain environmental conditions were required for the degradation of PAHs, e.g. sulfur oxidation, sulfate reducing, nitrate reducing and denitrifying condition.

This study and previous studies suggest that, in general environment, the degradation rate of PAHs in sediments were extremely slow, and PAHs in harbor sediments would persist for a long time.

4. MASS BALANCE MODEL

A mass balance model was applied to estimate quantitatively the mass balance of PAHs in Nagoya port.

(1) Outline of the model

This mass balance model was originally developed by Mackay et al. [21], and applied for PCB [22] and PAHs [23] fate in San Francisco Bay. **Fig. 12** shows the diagram of the model. The model quantitatively estimates inputs and outputs from the

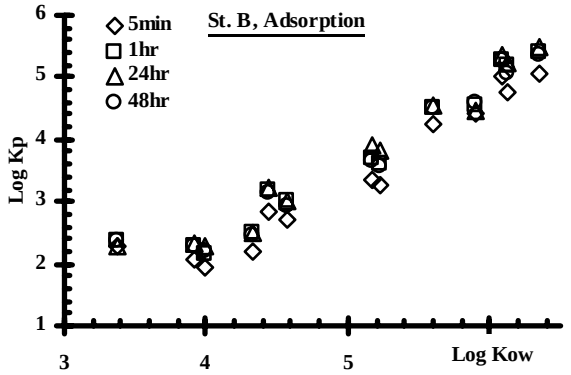

Fig. 5 Log K_p against Log K_{ow} with various stirred period in adsorption experiment

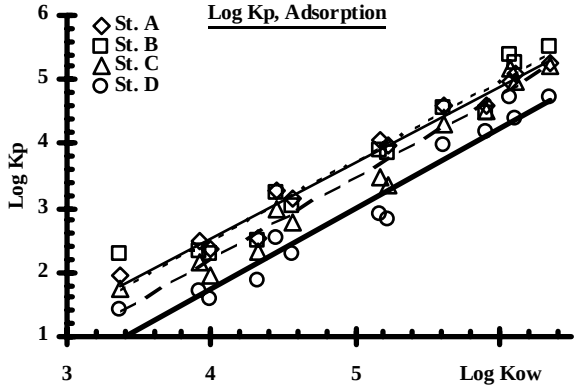

Fig. 6 Log K_p against Log K_{ow} at St. A to D in adsorption experiment

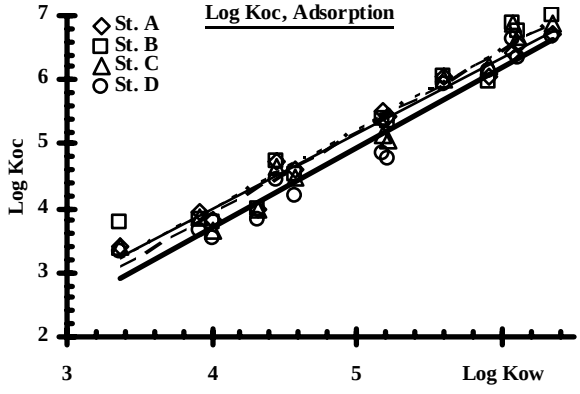

Fig. 7 Log K_{oc} against Log K_{ow} at St. A to D in adsorption experiment

Table 3 Log K_p, K_{om} *and* K_{oc} in adsorption experiments

	Log Kp	Log Kom	Log Koc
Naphthalene	1.84	2.76	3.49
Acenaphthylene	2.04	2.96	3.69
Acenaphthene	2.18	3.10	3.82
Fluorene	2.30	3.22	3.95
Phenanthrene	2.81	3.73	4.45
Anthracene	3.00	3.92	4.64
Fluoranthene	3.50	4.42	5.14
Pyrene	3.58	4.50	5.23
1,2-Benzanthracene	4.36	5.28	6.00
Chrysene	4.44	5.36	6.08
Benzo(b)fluoranthene	4.92	5.84	6.57
Benzo(k)fluoranthene	5.06	5.98	6.70
Benzo(a)pyrene	5.18	6.10	6.82

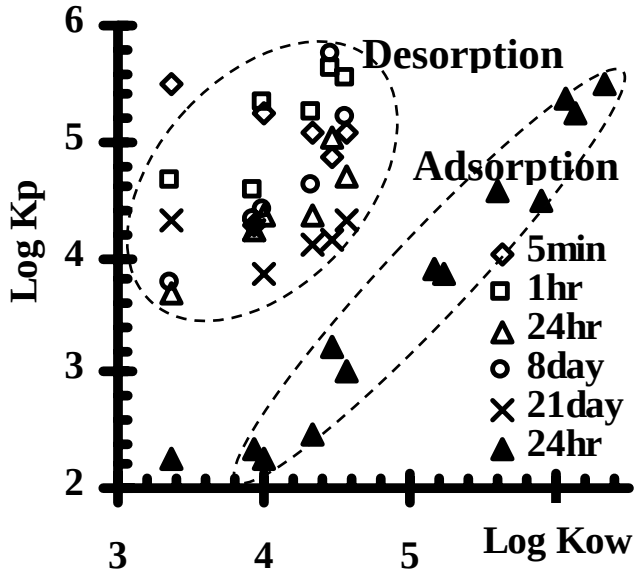

Fig.8 Log K_p against Log K_{ow} in desorption and adsorption experiment

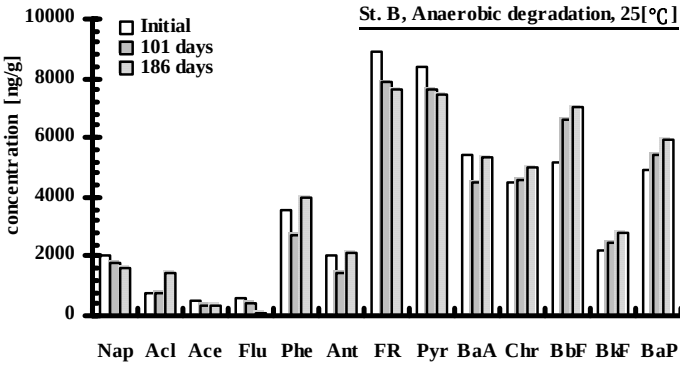

Fig. 9 PAHs concentration changes at St. B in anaerobic degradation experiment

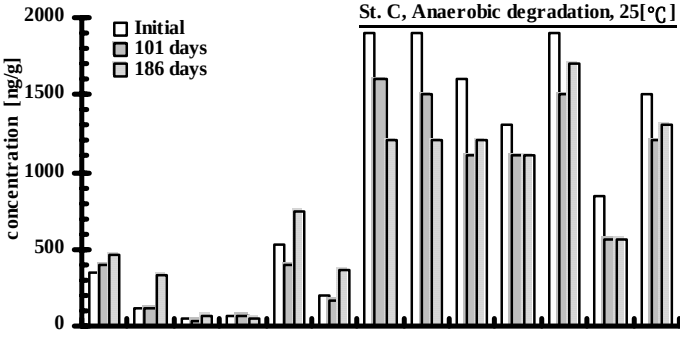

Fig. 10 PAHs concentration changes at St. C in anaerobic degradation experiment

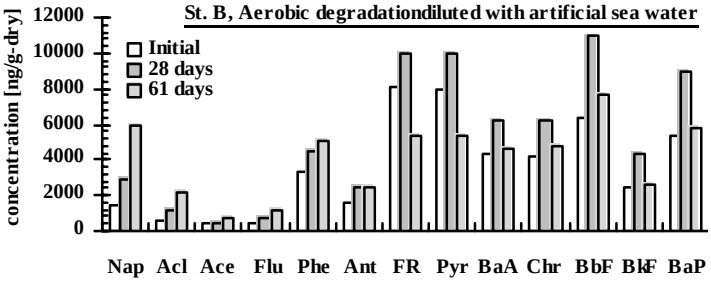

Fig. 11 PAHs concentration changes at St. B in aerobic degradation experiment

water and sediment compartments. These compartments are assumed to be mixed homogeneously. Port sediments are divided conceptually into an active sediment layer and buried sediment.

Inputs to the water column include external loads, resuspension of solid phase PAHs from sediment, and diffusion of dissolved PAHs from sediment. Outputs from the water column include volatilization to the atmosphere, outflow to the ocean, tidal exchange, deposition of solid phase PAHs to the active sediment layer, diffusion of dissolved PAHs to the active sediment layer, and degradation of PAHs in the water column.

Inputs to the active sediment layer include deposition of solid phase PAHs from the water column and diffusion of dissolved PAHs from the water column. Outputs from the active sediment layer include resuspension of solid phase PAHs to the water column, diffusion of dissolved PAHs to the water column, burial of solid phase PAHs as inaccessible deep sediment, and degradation of PAHs in the active sediment layer.

Mathematically, the model is based on two equations that describe the gains and losses of PAHs from the water column and the sediment layer:

$$\triangle M_w/\triangle t = L + (k_{sw1} + k_{sw2})\, M_s - (k_v + k_o + k_t + k_{ws1} + k_{ws2} + k_{rw})\, M_w \quad (2)$$

$$\triangle M_s/\triangle t = (k_{ws1} + k_{ws2})\, M_w - (k_{sw1} + k_{sw2} + k_b + k_{rs})\, M_s \quad (3)$$

M_w is the mass of PAHs in the water column include dissolved and solid phase. M_s is the mass of PAHs in the active sediment layer include dissolved and solid phase. Each "k" is a daily constant, indicating the proportion of present PAHs mass transformed and moved. The volatilization rate constant (k_v) was calculated as a function of Henry' law constant. The outflow rate constant (k_o) was a function of rate of water inflow to the port. The tidal exchange rate constant (k_t) was a function of rate tidal exchange. The solids settling rate constant (k_{ws1}) was calculated as a function of diameter of suspended solids using the Stokes equation. The water to sediment diffusion rate constant (k_{ws2}) was a function of diffusion coefficient of PAHs. The burial rate constant (k_b) was a function of sedimentation rate. The resuspension rate constant (k_{sw1}) was calculated as subtraction the sedimentation rate from the solids settling rate. The sediment to water diffusion rate constant (k_{sw2}) was a function of diffusion coefficient of PAHs. The degradation rate constant (k_{rw}, k_{rs}) was assumed to be zero. The external loading (L) was calculated value to balance the sum of M_w and M_s.

Input data for the model are summarized as shown in **Table 4**. The boundary of the box was determined at the breakwater i.e. inside of the box included St. A, B and C, while outside of the box included St. D. PAHs concentrations inside of the box in the model was the average value of St. A, B and C, and those outside of the box was the value of St. D. Target compounds are Naphthalene (Bi-cyclic) and Benzo(b)fluoranthene (Penta-cyclic). The rate constants were calculated for Naphthalene and Benzo(b)fluoranthene as shown in **Table 5**.

(2) Results and discussion

Fig. 13 shows the mass balance diagram with for Naphthalene in Nagoya port at steady state. The mass of Naphthalene in the water column was 11.7

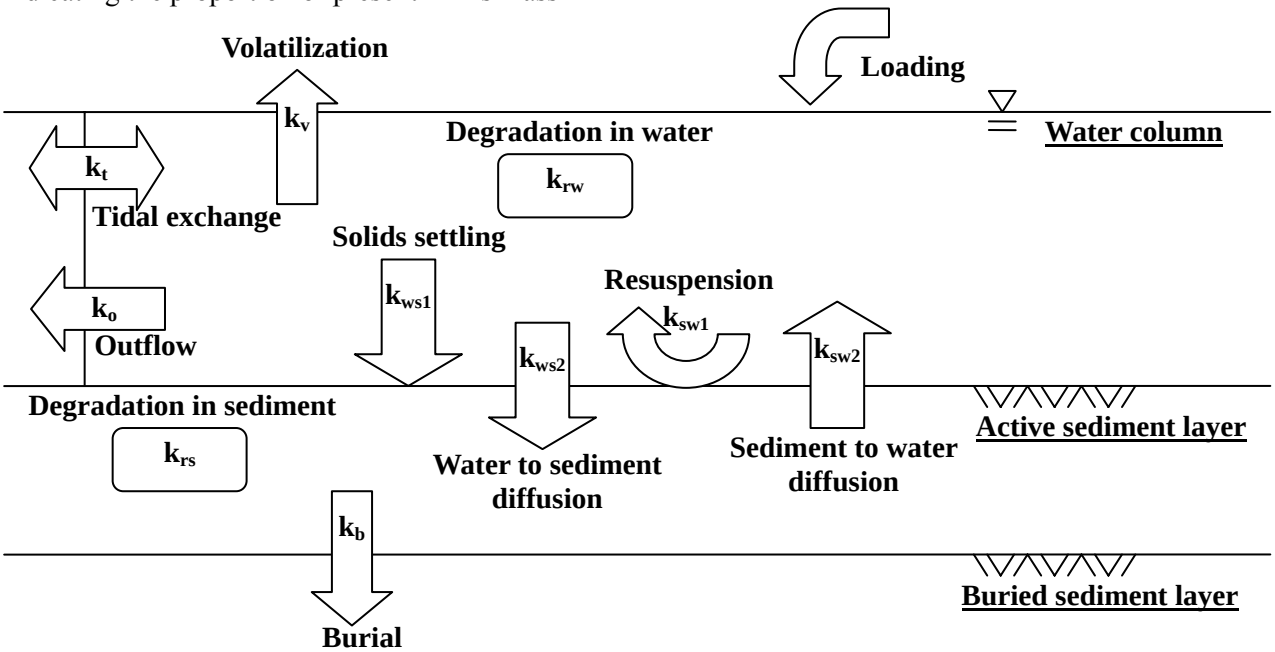

Fig. 12 Diagram of PAHs fate in Nagoya port showing processes included in the model.

Table 4 Input data for the model

Parameter	Symbol	unit	Ave. of St. A,B,C	St. D
Water surface area	A_w	m^2	32000000	-
Sediment surface area	A_s	m^2	32000000	-
Depth of water	H_w	m	14	-
Depth of active sediment layer	H_s	m	0.2	-
Water volume	V_w	m^3	448000000	-
Sediment volume of bay	V_s	m^3	6400000	-
Water temperature	T	℃	20	-
Water outflow	q	L/day	4410000000	-
Suspended solid in water column	SS_w	kg/L	0.0000107	-
Suspended solid in outer water	SS_o	kg/L	-	0.000001
Moisture ratio	θ	kg/L	0.71	-
Dry density of sediment	ρ_{ss}	kg/L	2.58	-
Sediment burial mass transfer coefficient	MTC_b	m/day	0.0000257	-
Solids settling rate	MTC_s	m/day	2.64	-
Average wind speed	U	km/hour	19.8	-
Average tidal exchange amount	V_t	L/day	83200000000	-
Concentration of solids in sediment	ρ_{ds}	kg/L	0.75	-
Resuspension flux of sediment solids	Res	kg/day	286000	-

Table 5 Rate constants for Nap and BbF in Nagoya port based on best estimates of model input data

	Symbol	unit	Naphthalene	Benzo(b)fluoranthene
Outflow rate constant	k_o	/day	0.00127	0.000165
Volatilization rate constant	k_v	/day	0.0242	0.00000513
Burial rate constant	k_b	/day	0.000128	0.000128
Tidal exchange rate constant	k_t	/day	0.162	0.183
Solids settling rate constant	k_{ws1}	/day	0.112	0.187
Water to sediment diffusion rate constant	k_{ws2}	/day	0.00783	0.000106
Resuspension rate constant	k_{sw1}	/day	0.0000599	0.0000599
Sediment to water diffusion rate constant	k_{sw2}	/day	0.00000823	0.000000540
Degradation loss rate in water	k_{rw}	/day	0.0	0.0
Degradation loss rate in sediment	k_{rs}	/day	0.0	0.0

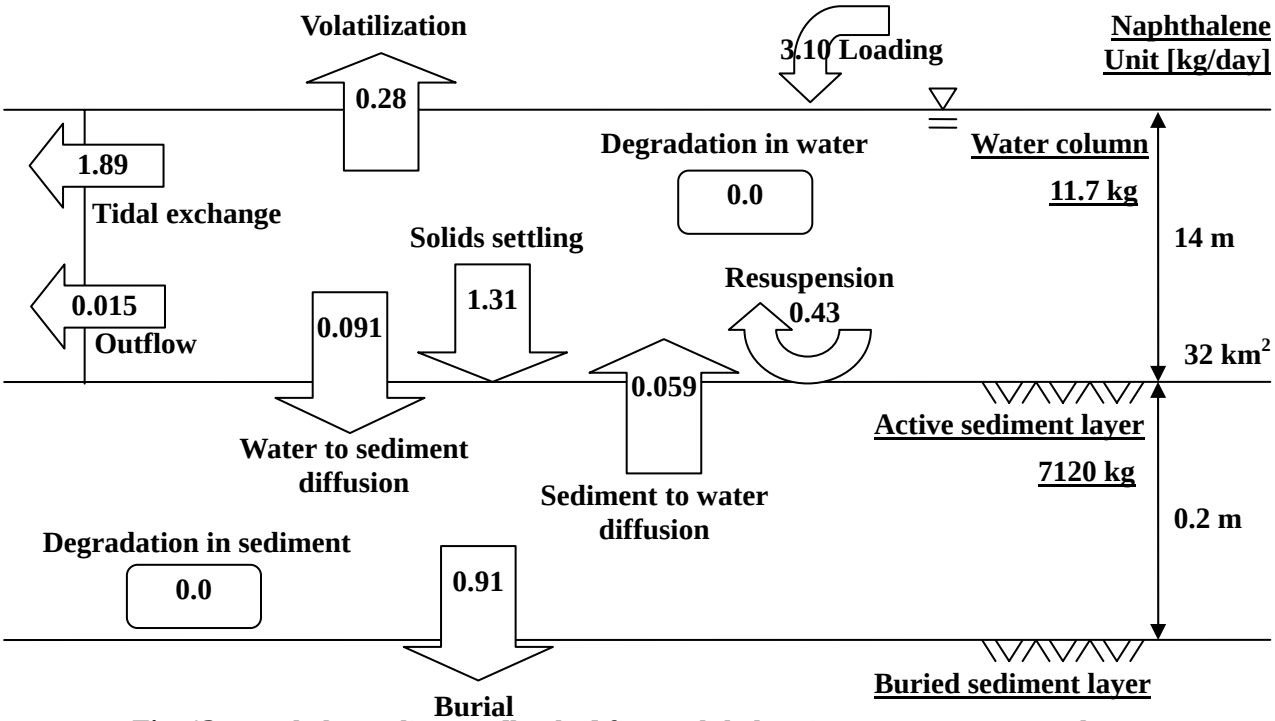

Fig. 13 Mass balance diagram [kg/day] for Naphthalene in Nagoya port at steady state

kg, and that in the active sediment layer was 7120 kg. The external loading of Naphthalene was calculated 3.10 kg/day. The resuspension of solid phase from sediment was 0.43 kg/day. Thus, the total Naphthalene inflow to the water column was approximately 3.53 kg/day. The solids settling of solid phase to the active sediment layer was 1.31 kg/day (37% of the total inflow). The outflow to the ocean that is the sum of the outflow and the tidal exchange was 1.90 kg/day (54% of the total inflow). The volatilization was 0.28 kg/day (8% of the total inflow). The diffusion from water to sediment was 0.091 kg/day, and the diffusion of the opposite direction was 0.059 kg/day, which shows water to sediment direction was predominant.

Fig. 14 shows the mass balance diagram with for Benzo(b)fluoranthene in Nagoya port at steady state. The mass of Benzo(b)fluoranthene in the water column was 12.2 kg, and in the active sediment layer was 12100 kg. The external loading of Benzo(b) fluoranthene was calculated 3.78 kg/day. The resuspension of solid phase from sediment was 0.72 kg/day. Thus, the total Benzo(b)fluoranthene inflow to the water column was approximately 4.50 kg/day. The solids settling of solid phase to the active sediment layer was 2.28 kg/day (50% of the total inflow). The outflow to the ocean that is the sum of the outflow and the tidal exchange was 2.23 kg/day. The volatilization was 0.000063kg/day (negligible small). The diffusion from water to sediment was 0.0013 kg/day (50% of total inflow), and the diffusion of the opposite direction was 0.065 kg/day, which shows sediment to water direction was predominant.

In Naphthalene case, 54% of the total inflow would be outflow, 8% would be volatilization, and contrast, Benzo(b)fluoranthene case, 50% of the total inflow would be outflow, and 50% would be solids settling to sediment. Therefore, the more ring-number compounds are the more sedimentation in the port.

In general, the more ring-number compounds are more toxic, and considered to have more environmental effects. It is an implication for chemical substances management in ports and harbors that the ratio of the sedimentation to the total loading in ports and harbors increases with the ring-number of PAHs, and they persist in sediments for a long time due to there low degradability.

5. CONCLUSIONS

To clarify the environmental fate of PAHs, the field observation in Nagoya port and the laboratory experiments using Nagoya port sediments were conducted. The data obtained from the field observation and the laboratory experiments were used to calculate quantitatively the mass balance of PAHs in Nagoya port. The results were summarized as follows;

1) PAHs were detected at relatively high levels in Nagoya port, $\sum_{13}$PAHs were 580-51000 ng/g-dry. $\sum_{13}$PAHs at St. B was exceeded the ERM that is the guideline value used in U.S.

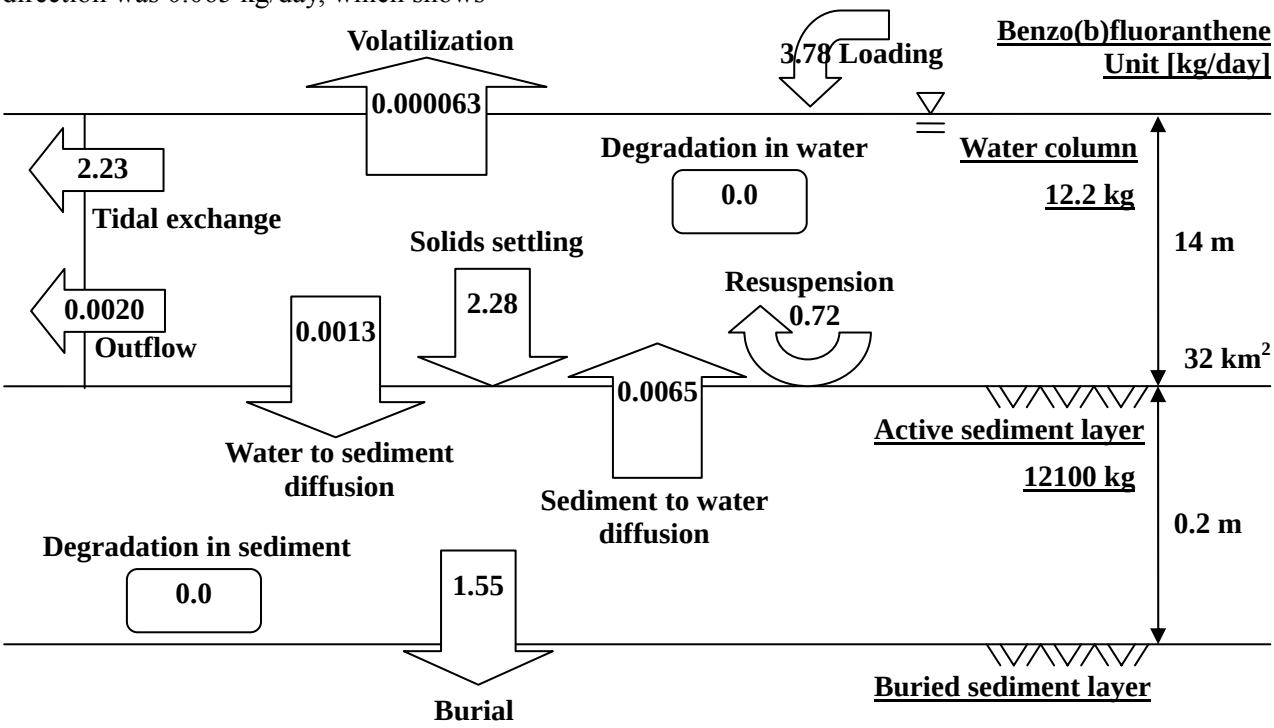

Fig. 14 Mass balance diagram [kg/day] for Benzo(b)fluoranthene in Nagoya port at steady state

2) PAHs isomer pair ratios showed that combustion of fossil fuel/petroleum was a major source of PAHs to Nagoya port sediments, with lesser contribution of direct petroleum input.

3) The adsorption capacity of PAHs in sediment was related to water-octanol partition coefficient of the PAHs and TOC of sediments.

4) K_p obtained from the desorption experiment was 30-100 times greater than that obtained from the adsorption experiment. PAHs that once adsorbed to sediments would not be released, even if sediments were diluted in sea water due to resuspension.

5) The degradation rate of PAHs in sediments were extremely low, and the PAHs in harbor sediments would persist for a long time.

6) As to the final destination of PAHs, the ratio of the sedimentation to the total loading in ports and harbors increases with the ring-number of PAHs, and they persist in sediments for a long time due to there low degradability.

REFERENCES

[1] Toshiharu Hirose, Keiko Morito, Ryoichi Kizu, Akira Toriba, Kazuichi Hayakawa, Sumito Ogawa, Satoshi Inoue, Masami Muramatsu, and Yukito Masamune. Estorogenic/Antiestrogenic Avtivities of Benzo(a)pyrene Monohydroxy Derivatives. Journal of Health Science 2001, 47 (6), 552-558.

[2] Makiko Kamiya, Akira Tobira, Yu Onoda, Ryuichi Kizu, Kazuichi Hayakawa. Evaluation of estrogenic activities of hydroxylated polycyclic aromatic hydrocarbons in cigarette smoke condensate. Food and Chemical Toxicology 2005, 43, 1017-1027.

[3] Heike Kaupp, and Michael S. Mclachlan. Gas/Particulate partitioning of PCDD/Fs, PCBs, PCNs and PAHs. Chemosphere 1999, Vol. 38, No. 14, 3411-3421.

[4] R.K. Aryal, H. Furumai, F. Nakajima, M. Boller. Dynamic behavior of fractional suspended solids and particle-bound polycyclic aromatic hydrocarbons in highway runoff. Water Research 2005, 39, 5126-5134.

[5] Yamazaki Tomohiro. Environmental Behavior of Organotin Compounds in Harbor Sediments. Doctor thesis, Graduate School of Environment and Information Sciences, Yokohama National University, 2006. (in Japanese)

[6] Xiao-Jun Luo, She-Jun Chen, Bi-Xian Mai, Qing-Shu Yang, Guo-Ying Sheng, Jia-Mo Fu. Polycyclic aromatic hydrocarbons in suspended particulate matter and sediments from the Pearl River Estuary and adjacent coastal areas, China. Environmental Pollution 2006; 139: 9-20.

[7] Gene J. Zheng, Ben K.W. Man, James C.W Lam, Michael H.W. Lam, Paul K.S. Lam. Distribution and sources of polycyclic hydrocarbons in the sediment of a sub-tropical coastal wetland. Water Research 2002, 36: 1457-1468.

[8] Yoshinori Ikenaka, Heesoo Eun, Eiki Watanabe, Fujio Kumon, Yuichi Miyabara. Estimation of sources and inflow of dioxins and polycyclic aromatic hydrocarbons from the sediment core of Lake Suwa, Japan. Environmental Pollution 2005, 138: 529-537.

[9] Daniel R. Oros, John R.M. Ross, Robert B.Spies, Thomas Mumley. Polycyclic aromatic hydrocarbon (PAH) contamination in San Francisco Bay: A 10-year retrospective of monitoring in an urbanized estuary. Environmental Research 2007, 105: 101-118.

[10] Nobuyuki Yamashita, Kurunthachalam Kannan, Takashi Imagawa, Daniel L. Villeneuve, Shinya Hashimoto, Akira Miyazaki, John P. Giesy. Vertical Profile of Polychlorinated Dibenzo-p-dioxin, Dibenzofurans, Naphthalene, Biphenyls, Polycyclic Aromatic Hydrocarbons, and Alkylphenols in a Sediment Core from Tokyo Bay, Japan. Environmental Science and Technology 2000, 34: 3560-3567.

[11] Hiroshi Moriwaki, Kenshi Katahara, Osamu Yamamoto, Joji Fukuyama, Toshikazu Kamiura, Hideo Yamazaki, Shusaku Yoshikawa. Historical trends of polycyclic aromatic hydrocarbons in the reservoir sediment core at Osaka. Atmospheric Environment 2005, 39: 1019-1025.

[12] National Oceanic and Atmospheric Administration. Sediment Quality Guideline developed for the National Status and Trends Program. National Oceanic and Atmospheric Administration, 1999.

[13] Kunlei Liu, Wei Xie, Zheng-Bao Zhao, Wei-Ping Pan, and John T. Riley. Investigation of Polycyclic Aromatic Hydrocarbons in Fly Ash from Fluidized Bed Combustion System. Environmental Science and Technology 2000, 34, 2273-2279.

[14] Linsey C. Marr, Thomas W. Kirchstetter, Robert A. Harley, Antonio H. Miguel, Susanne V. Hering, and S. Katharine Hammond. Characterization of Polycyclic Aromatic Hydrocarbons in Motor Vehicle and Exhaust Emissions. Environmental Science and Technology 1999, 33, 3091-3099.

[15] Mark B. Yanker, Robie W. Macdonald, Roxanne Vingarzan, Reginald H. Mitchell, Darcy Goyette, Stephanie Sylvestre. PAHs in the Fraster River basin: a critical appraisal of PAH ratios as indicators of PAH source and composition. Organic Geochemistry 2002, 33: 489-515.

[16] Dan L. Mcnally, James R. Mihelcic, and Donald R. Lueking. Biodegradation of Three- and Four-Ring Polycyclic Aromatic Hydrocarbons under Aerobic and Denitrifing Conditions. Environmental Science and Technology 1998, 32, 2633-2639.

[17] Rainer U. Meckenstock, Michael Safinowski, and Christian Griebler. Anaerobic degradation of polycyclic aromatic hydrocarbons. FEMS Microbiology Ecology 2004, 49, 27-36.

[18] Mary M. Rothermich, Lory A. Hayes, and Derek R. Lovley. Anaerobic, Sulfate-Dependent Degradation of Polycyclic Aromatic Hydrocarbons in Petroleum-Contaminated Harbor Sediment. Environmental Science and Technology 2002, 36, 4811-4817.

[19] C. Quantin, E.J. Joner, J.M. Portal, and J. Berthelin. PAH dissipation in a contaminated river sediment under oxic and anoxic conditions. Environmental Pollution 2005, 134, 315-322.

[20] L. Lei, A.P. Khodadoust, M.T. Suidan, and H.H. Tabak. Biodegradation of sediment-bound PAHs in field-contaminated sediment. Water Research 2005, 39, 349-361.

[21] Donald Mackay and Brendan Hickie. Mass balance model of source apportionment, transport and fate of PAHs in Lac Sint Louis, Quebec. Chemosphere 2000, 41, 681-692.

[22] Jay A. Davis. The long-term fate of polychlorinated biphenyls in San Francisco Bay (USA). Environmental Toxicology and Chemistry, Vol. 23, No. 10, 2004, 2396-2409.

[23] Ben K. Greenfield, Jay A Davis. A PAH fate model for San Francisco Bay. Chemosphere 60, 2005, 515-530.